Integrating GIS-Based Spatial Analysis and Structural Modeling for the Adaptive Reuse of the Santa Chiara Dam

Enrica Vecchi(✉) and Marco Zucca

Department of Civil, Environmental Engineering and Architecture, University of Cagliari, Cagliari 09123, Italy
{enrica.vecchi,marco.zucca2}@unica.it

Abstract. Adaptive reuse of historic hydraulic infrastructures requires precise geometric reconstruction to enable reliable structural assessment and design-oriented evaluations. This study presents an integrated workflow combining GIS-based spatial analysis and structural modeling, applied to the Santa Chiara Dam, a decommissioned early 20th-century gravity–multiple-arch dam located on the Tirso River (Sardinia, Italy).

A key challenge addressed in this work is the lack of direct bathymetric information for the partially submerged reservoir basin. Existing high-resolution LiDAR-derived Digital Terrain Models (DTMs, 1 m resolution) provided by the Sardinian Geoportal capture only the water surface, leaving the underlying morphology undefined. For partially submerged dams, even an approximate reconstruction of the reservoir basin is essential, not only for documenting the structure itself but also for defining the spatial context required for reliable structural assessment and load distribution analysis. To overcome this limitation, a dedicated integrated workflow was developed, combining GIS-based spatial analysis with structural modeling. The workflow includes: (i) extraction and clipping of external terrain morphology; (ii) slope analysis of surrounding banks; (iii) geometric reconstruction of transition zones through transversal profiles and linear gradient assumptions; (iv) generation of a continuous terrain model via TIN interpolation and raster merging; and (v) non-linear finite element analysis of the dam structure using Midas FEA software.

Results indicate an overall satisfactory structural response, with limited displacements and predominantly compressive stress states, while highlighting localized tensile stress concentrations at arch–buttress interfaces.

The proposed workflow demonstrates the value of integrating GIS-based spatial analysis with structural modeling for heritage hydraulic structures, facilitating both accurate structural evaluation and sustainable adaptive reuse strategies. The methodology is transferable to similar historical infrastructures where incomplete topographic or bathymetric data limit conventional assessment approaches.

Keywords: Adaptive Reuse · Historic Dams · GIS · Spatial Analysis · Structural Modeling · Digital Terrain Model · Finite Element Analysis · Cultural Heritage · Sardinia

© The Author(s), under exclusive license to Springer Nature Switzerland AG 2027
O. Gervasi et al. (Eds.): ICCSA 2026 Workshops, LNCS 16766, pp. 37–53, 2027.
https://doi.org/10.1007/978-3-032-30539-8_3

1 Introduction

The rehabilitation and reuse of existing infrastructure have become one of the most important and timely research topics in civil and environmental engineering, particularly in the context of aging assets and the growing demand for sustainable construction strategies. Over the past decades, numerous projects have therefore focused on the rehabilitation of large-scale infrastructures of significant historical and cultural value, with the aim of extending their service life while preserving their structural and architectural identity [1–3]. Among these infrastructures, dams stand out because of their strategic importance, structural complexity, and the potential consequences associated with their deterioration or abandonment. Indeed, even when no longer operational, many of these structures constitute valuable elements of industrial heritage, providing important evidence of past engineering practices and technological development. For this reason, the assessment, preservation, and possible rehabilitation of such infrastructures have become key topics in both structural and conservation engineering [4, 5].

Historical dams are often characterized by complex geometries that are difficult to reconstruct, particularly in portions that remain permanently submerged, where direct inspection and geometric documentation are typically limited. Furthermore, the wetdry cycles affecting exposed areas may lead to significant material degradation, influencing both primary and secondary structural elements. Different approaches have been developed to address these challenges, integrating geometric reconstruction with advanced structural analysis methods.

Previous studies have explored different modeling strategies. In [6], the structural performance of a large arch dam was evaluated under both static and dynamic loads, with particular attention to joint movements. Fedele et al. [7] proposed a new approach to assess the influence of the alkali-silica reaction and the presence of diffused microcracking on structural performance of existing concrete dams, depending on the age of the structure. A numerical model, based on the Discrete Element Method (DEM), was proposed in [8] to investigate failure mechanisms involving the dam body and the damrock interface. In particular, dedicated tools for the analysis of masonry gravity dams have been developed, using the Guilhofrei Dam as a case study. Nguyen-Tuan et al. [9] developed a coupled thermo-hydro-mechanical model for masonry dams optimized through parallel computation. Robles and Pena [10] analyzed the influence of masonry mechanical properties on the structural behavior of masonry dams. Results of parametric analyses identified tensile strength as a key parameter governing structural response. The study reported in [11] investigates the condition and potential reuse of stone masonry from the Kada Dam after 46 years of service, highlighting that the blocks preserve sufficient residual strength to be employed in new gravity dams' construction.

In this study, the structural behavior of the Santa Chiara Dam on the Tirso River (Sardinia) is investigated starting from a GIS-based reconstruction of the riverbed geometry. A dedicated workflow integrating GIS-based spatial analysis, supported by custom python routines, with structural modeling is proposed. Completed in 1924 based on the design by Luigi Kambo and Angelo Omodeo, the dam played a key role in the economic and social development of the region and is currently the subject of a rehabilitation program.

The paper is organized as follows. Section 2 describes the dam from a historical, structural, and geological perspective. Section 3 presents the methodology used for the reconstruction of the Digital Terrain Model (DTM). Section 4 describes the Finite Element Modeling (FEM) and discusses the main results of the non-linear static analysis, considering the safety requirements imposed by the rehabilitation project. Finally, Sect. 5 summarizes the main findings and outlines directions for future developments.

This integrated approach enables the definition of a consistent geometric framework linking terrain morphology, hydraulic context, and structural configuration of the dam, supporting both structural assessment and the sustainable management of historical hydraulic infrastructures.

2 Santa Chiara Dam

2.1 Brief Historical Notes

The Santa Chiara Dam is located in central Sardinia (Italy), in the Province of Oristano, within the municipality of Ulà Tirso, along the Tirso River. Construction took place between 1918 and 1924, although initial design studies for the dam and its artificial reservoir date back to 1912 (Fig. 1). The project was conceived by the engineer Angelo Omodeo and executed by the company *"Imprese Idrauliche ed Elettriche"*, with the aim of flood regulation along the Tirso River, hydroelectric power generation, and irrigation to the Campidano plain. After the dam was completed, the upstream artificial reservoir was named Lake Omodeo to honor the project designer.



Fig. 1. Santa Chiara dam today.

The artificial reservoir was initially realized as a water storage system intended to support irrigation, but the project was subsequently revised and adapted to include hydroelectric power generation. This required increasing the reservoir capacity and relocating the dam to exploit a higher hydraulic head and improve the efficiency of the power plant.

Construction works of the gravity dam began in 1918 under engineer Luigi Kambo's supervision and continued until 1924. During foundation excavation, a tuffaceous substratum was discovered, which was neither sufficiently compact nor mechanically resistant to support the stresses predicted at the dam's base by the original design. This condition would have required substantially larger concrete volumes, making the original gravity dam design economically unfeasible. In agreement with Kambo, Omodeo and Giulio Dolcetta proposed significant modifications, ultimately constructing a multiple-arch dam 260 m long and 70 m high (Fig. 2).

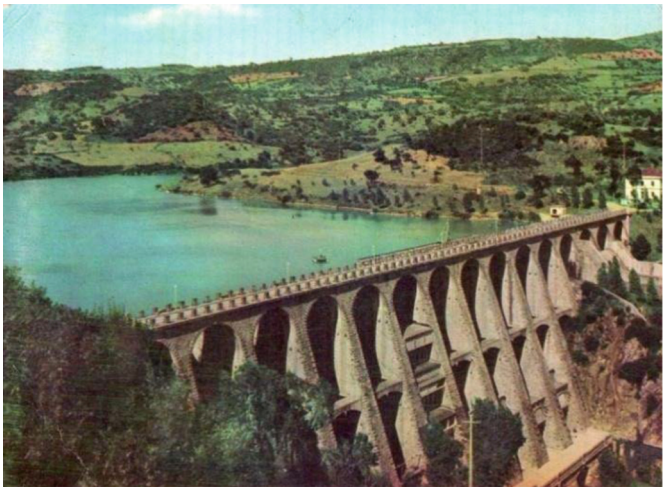

Fig. 2. Santa Chiara Dam during its first year of operation [12].

The project was completed in 1924 and officially inaugurated on 28 April of the same year. The dam remained in operation until 1968, when structural issues in the buttresses led to operational limitations. Although a replacement dam downstream was considered to increase water storage capacity, Santa Chiara was formally decommissioned only in 1997 and fully taken out of service by 2000.

2.2 Structural and Geological Configuration

The dam is a composite masonry-concrete structure, consisting of 17 spans with a clear span of 15 m each. The maximum height from the foundation is 61 m, reaching an elevation of 109 m above sea level. The structural layout follows the typical scheme of gravity dams.

The buttresses are reinforced by a four series of semicircular arches with a span of 12.5 m, above which a 6 m-wide roadway runs at a constant elevation of 112 m a.s.l. Figure 3 illustrates the plan view of the dam, indicating the main structural elements.

The buttresses and arches are constructed of trachyte masonry with cement mortar joints, whereas the downstream shells are made of concrete. Original design documentation indicates a mortar composition with 300 kg/m^3 cement, a compressive strength

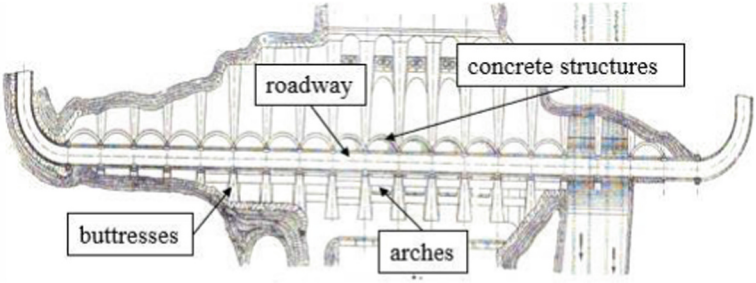

Fig. 3. Dam plan view.

of 27 MPa, and a tensile strength of 0.35 MPa after 180 days. After 28 days, the mortar exhibits a compressive strength of 13.5 MPa and a tensile strength of 0.15 MPa, while the concrete can be considered equivalent to a C25/30 strength class with a unit weight equal to 25 kN/m^3. Trachyte masonry shows a compressive strength of 3 MPa, tensile strength of 0.3 MPa, and a unit weight of 22 kN/m^3, as reported in [13]. Table 1 summarizes the key mechanical parameters of materials used in the main structural elements.

Table 1. Mechanical properties of main structural elements

Element	Material	Elastic Modulus [MPa]	Compressive strength [MPa]	Tensile strength [MPa]
Buttresses Arches Shells	trachyte trachyte concrete	2400 2400 29961	3 3 30	0.3 0.3 3

From a geological and lithological perspective, the study area is characterized by Cenozoic volcanic rocks, mainly Upper Oligocene to Middle Miocene volcanites, locally associated with a late Hercynian magmatic complex of intrusive and volcanic origin. The foundation bedrock is primarily constituted by compact trachyte flows, overlain in places by continental and marine sediments from the Upper Paleocene to Pliocene. The geological setting is further influenced by a Cenozoic post-Hercynian fault system that crosses a significant portion of the reservoir approximately perpendicular to its main axis, representing a major structural discontinuity within the rock mass.

The surface stratigraphy includes vesicular and compact basalts, trachytic tuffs, and compact trachytes, which constitute the primary volcanic units of the area. The wider catchment basin is mainly composed of granites and crystalline schists, which are particularly prone to weathering and thus contribute to the formation of a weathered mantle and localized alluvial deposits. In the western sector, ancient trachytes form the basal substratum, while basaltic lava flows create plateau structures occasionally overlaying them, sometimes associated with volcanic tuff deposits. Alluvial areas on the plateaus mainly consist of clayey-sandy soils with rounded quartz pebbles, whose size and abundance progressively decrease toward the coastal plain.

3 Gis-Based Spatial Analysis

This chapter describes the methodology adopted to reconstruct a simplified model of the riverbed in the area surrounding the Santa Chiara dam. The reconstruction is based on the integration of publicly available geospatial datasets, historical drawings, technical documentation, geometric assumptions, and information derived from the literature, all combined within a GIS environment to produce a consistent and reproducible representation of the reservoir basin. The procedure was implemented using the opensource software QGIS (version 3.34) [14] supported by custom python scripting and is fully reproducible and transferable to similar case studies characterized by incomplete geomorphological data. The following sections first present the available UAV photogrammetric dataset (Sect. 3.1), then discuss the limitations of publicly available Digital Elevation Models in representing submerged terrain (Sect. 3.2) and finally describe the simplified reconstruction of the riverbed geometry based on GIS analysis and geometric assumptions (Sect. 3.3).

3.1 UAV Photogrammetric Model of the Emerged Structure

A recent UAV-based photogrammetric model of the dam and its surrounding environment was available for this study, providing a detailed three-dimensional representation of the structure and adjacent terrain. The dataset was acquired using a DJI Mavic 3 platform equipped with an onboard camera featuring a nominal focal length of 4.4 mm (equivalent to 24 in 35 mm format). A total of 939 images were collected through combined nadir and oblique flight configurations.

The images were processed using a Structure-from-Motion workflow in Agisoft Metashape (version 2.2.2) [15]. Georeferencing was performed using 26 Ground Control Points (GCPs) surveyed with GNSS in NRTK mode, achieving an accuracy on the order of 3–4 cm in the Northing and Easting and about 5 cm in the height. The main products include a dense point cloud (Fig. 4) and a high-resolution orthophoto.

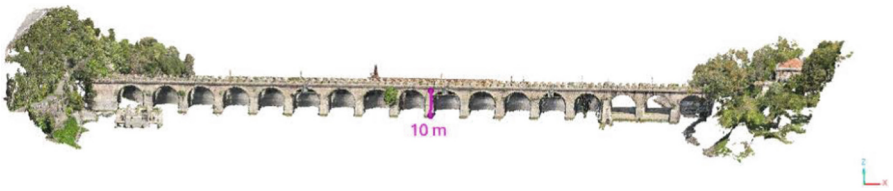

Fig. 4. Dense point cloud derived from UAV photogrammetry (SfM), georeferenced using GNSS-surveyed GCPs. The model provides a detailed 3D representation of the visible portions of the dam and surrounding terrain.

Although the photogrammetric dataset provides a detailed three-dimensional representation of the visible portions of the dam and surrounding terrain, it does not capture reliable elevation information for the submerged riverbed due to the presence of water

surfaces and their significant seasonal variability [16]. This limitation is inherent to optical survey techniques, as water bodies prevent the reconstruction of underlying terrain features using standard SfM approaches [17].

Within the proposed workflow, the UAV model is therefore primarily used to support the geometric characterization of the exposed structure and the spatial interpretation of the study area, serving as a complementary dataset.

3.2 Limitations of Publicly Available DTMs

A reliable representation of the riverbed is essential for the structural assessment of partially submerged hydraulic infrastructures such as the Santa Chiara Dam. Indeed, since the present study relies on historical drawings and technical documentation, reconstructing the submerged riverbed is necessary to correctly define the dam geometry and its interaction with the surrounding terrain. This aspect is particularly relevant in heritage engineering applications, where incomplete or indirect data must be integrated to obtain consistent structural models [18]. Moreover, the reconstructed basin is crucial for setting boundary conditions and loading scenarios in the finite element model, enabling a realistic representation of hydrostatic pressure along the dam body.

However, none of the publicly available Digital Elevation Model datasets for the study area provide direct information on the morphology of the riverbed beneath the water surface, as they only capture the water surface at the time of acquisition. It is worth noting that this limitation is common to many open-access geospatial datasets, including regional geoportals and national mapping services, which are typically optimized to represent emerged terrain rather than submerged environments. This issue is also inherent to DTMs derived from standard airborne LiDAR surveys, as laser pulses are unable to penetrate water unless specifically designed for bathymetric measurements [19, 20]. On the other hand, while dedicated bathymetric datasets and hydrographic surveys are available for major rivers and large water bodies (e.g., USGS bathymetric surveys [21], NOAA hydrographic survey data [22], and GEBCO global bathymetry [23])), they are typically absent for smaller reservoirs such as the one considered in this study [24]. In such cases, information on water bodies is often limited to planimetric data (e.g., shoreline digitization), with no associated depth information, unless dedicated field surveys are conducted.

Within this context of limited data availability, the primary geospatial information for the Santa Chiara Dam area was obtained from the Geoportal of the Autonomous Region of Sardinia [25]. Among the available datasets, the high-resolution Digital Terrain Model (DTM) produced from airborne LiDAR surveys in 2010 by the Italian Ministry for the Environment was chosen for this study. The DTM belongs to the "DTM River Bands" collection, with a spatial resolution of 1 m, and is referenced to the ETRF2000 / UTM Zone 32 N coordinate system (EPSG:6707), the official national reference system in Sardinia.

As mentioned, this dataset, acquired for topographic and hydraulic risk assessment purposes, represents water-covered areas as flat surfaces corresponding to the water level, without including bathymetric information. This limitation is illustrated in Fig. 5, which shows the regional DTM (a) together with an elevation profile extracted across the reservoir using the QGIS Profile Tool plugin (b). While the surrounding terrain

exhibits realistic topographic variability, the profile within the reservoir remains nearly constant, clearly indicating that the model represents the water surface rather than the actual riverbed.

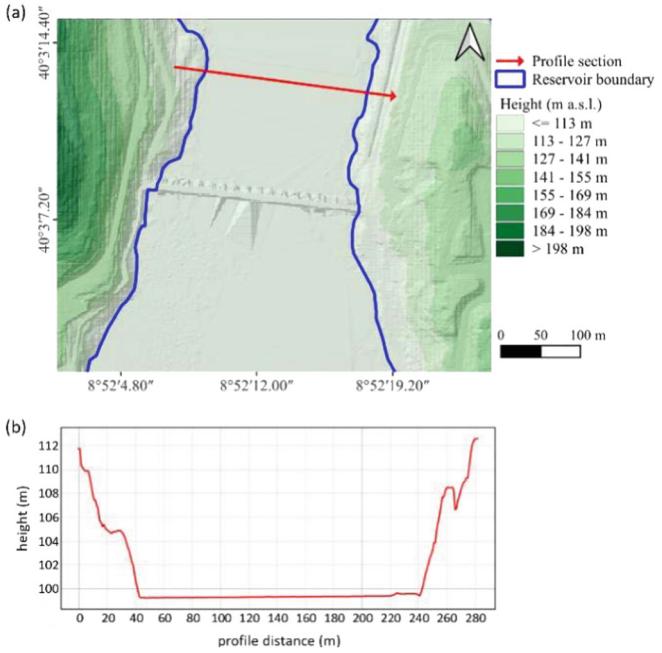

Fig. 5. Regional LiDAR-derived DTM of the study area, showing the location of the extracted profile and the reservoir boundary; (b) corresponding elevation profile extracted using the Qgis Profile Tool plugin. Elevations are expressed as orthometric heights (m a.s.l.), and coordinates are referenced to the WGS84 system (EPSG:4326).

To address this issue, which prevent the dataset from being directly used due to misleading heights, water-covered portions of the DTM were excluded by manually digitizing the reservoir boundary from recent satellite imagery. This allowed a clear separation between areas reliably captured by LiDAR and sectors affected by water-surface representation. The resulting clipped DTM was then used to derive a slope map, which provided an initial characterization of the terrain and informed the geometric assumptions for reconstructing the submerged basin (Fig. 6).

3.3 Simplified Reconstruction of the Riverbed

Based on the pre-processed terrain data described in the previous section, a simplified reconstruction of the reservoir basin was developed using geometric assumptions and other available information. The adopted configuration was intended as an approximate representation of the submerged morphology rather than a fully representative geomorphological model of the actual terrain. This approach was considered a reasonable

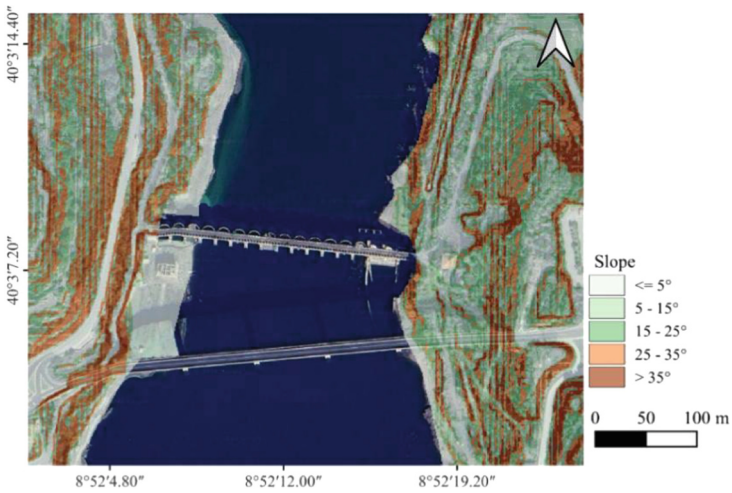

Fig. 6. Slope map derived from the LiDAR-based DTM provided by the Sardegna Geoportal. Grid coordinates are aligned to the WGS84 reference system (EPSG:4326).

compromise between realism, data availability, and methodological feasibility for the purposes of the present study.

The deepest portion of the reservoir basin was represented as a uniform-elevation surface, corresponding to the central flat portion of the riverbed. According to the original technical documentation, this elevation was set to 50 m above mean sea level [12]. The central polygon was rasterized within the GIS environment, assigning the constant elevation value to each cell. The resulting raster was generated at 1 m spatial resolution and in the same coordinate reference system as the original LiDAR-derived DTM, ensuring seamless integration with the surrounding terrain. This simplified flat-bottom surface serves as the foundation for defining the lateral transition zones connecting the riverbed to adjacent terrain (Fig. 7a).

The lateral sections of the basin were reconstructed using a simplified geometric approach. The cross-section was idealized as an isosceles trapezoid, with linear slopes bridging the elevation difference between the riverbed and the surrounding terrain. The definition of representative slope values was therefore a key step in ensuring a geometrically consistent and physically plausible model.

Preliminary analyses included the extraction of slope gradients along multiple transects derived from the DTM. However, to reduce the influence of local topographic irregularities and ensure consistency with historical design information, a simplified geometric approach based on known reservoir dimensions was ultimately adopted.

According to this approach, the river's total width (approximately 250 m) and the width of the central flat-bottom region (100 m) define two symmetrical transition zone of 75 m on each side. The elevation difference between the surrounding terrain (≈99 m a.s.l.) and the riverbed (50 m a.s.l.) results in a vertical drop of 49 m. Assuming a linear profile, the slope of the riverbanks was defined as the ratio between vertical and horizontal distance, resulting in an inclination of approximately 33° (about 65%).

This value was considered representative of the overall basin geometry, as it provides a robust approximation that is less affected by local topographic noise compared to purely data-driven slope estimations [26]. Based on this assumption, the eastern and western transition zones were delineated by offsetting the river boundary line by a uniform distance of 75 m, resulting in two distinct polygons representing the sloping riverbanks.

A continuous elevation surface for the transition zones was generated using a transect-based workflow developed through custom Python scripts. Points were initially sampled along the river boundary at 1 m intervals, and each point was assigned the elevation of the nearest terrain DTM pixel, representing the interface between emerged terrain and water-covered areas.

From these boundary points, transects extending toward the interior of the reservoir were generated. Along each transect, additional points were distributed at 0.5 m intervals, and their elevations were linearly interpolated from the terrain level down to the riverbed elevation, following the predefined slope.

The resulting sets of points, representing distributed elevation values along the transition zones, were interpolated using a Triangulated Irregular Network (TIN) algorithm, to generate continuous raster surfaces at 1 m resolution (compatible with the original LiDAR-derived terrain model). Figure 7 illustrates the intermediate raster layers used in the reconstruction process, including the constant-depth central riverbed (a) and the interpolated transition surfaces derived from the transect-based procedure on the eastern and western sides (b).

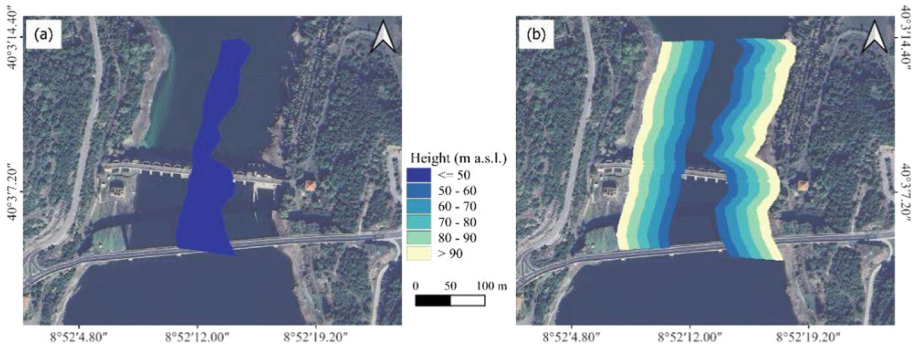

Fig. 7. Intermediate raster layers used for the reconstruction of the reservoir basin: (a) constantdepth central riverbed; (b) interpolated transition surfaces for the eastern and western banks generated from transect-based elevation points. Elevations are expressed as orthometric heights in meters above sea level (m a.s.l.), and grid coordinates are aligned to the WGS84 reference system (EPSG:4326).

The raster datasets representing the central riverbed and the two transition zones were then spatially aligned to ensure identical grid size, origin, and coordinate reference system. Alignment was performed using GDAL tools, enforcing uniform 1 m resolution and consistent grid anchoring. Once aligned, the rasters were merged into a single continuous DTM representing the reconstructed basin. NoData values were carefully handled,

and local interpolation was applied where necessary to eliminate discontinuities and ensure smooth transitions between surfaces.

The final reconstructed DTM provides a continuous and coherent representation of the basin, suitable for both geometric analysis and integration into structural numerical modeling workflows. To facilitate this integration, the DTM was further processed within the GIS environment to extract contour lines describing the riverbed geometry, as shown in Fig. 8.

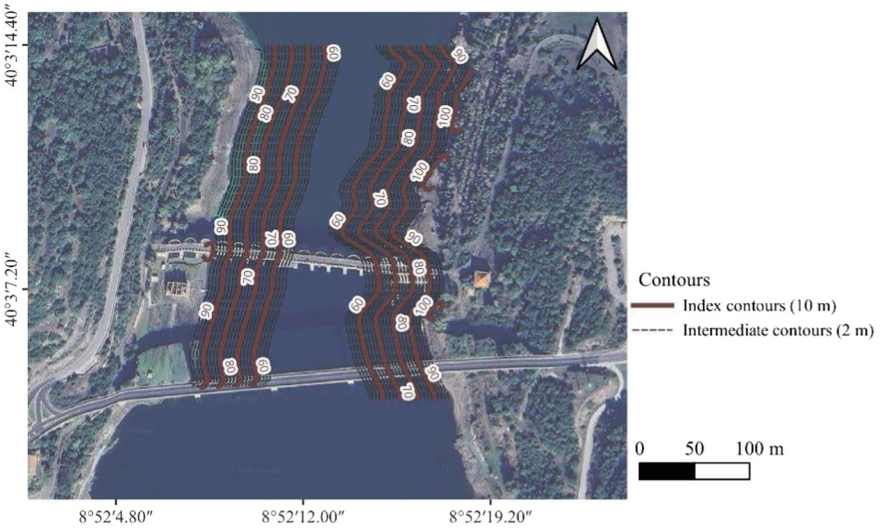

Fig. 8. Contour lines generated from the reconstructed DTM. Elevations are given as orthometric heights in meters above sea level (m a.s.l.), and grid coordinates are aligned to the WGS84 reference system (EPSG:4326).

4 Structural Modelling and Numerical Analysis

4.1 Geometry Reconstruction

The geometric reconstruction of the dam was achieved by integrating data derived from the UAV photogrammetric survey with the available historical documentation. These sources together provided the basis for generating a 3D model of the Santa Chiara Dam within a commercial modelling environment [27]. In particular, the main structural components (buttresses, arches, shells, and slabs) were represented using solid elements, allowing the complex geometric configuration typical of this type of structure to be reproduced with adequate accuracy. Since the initial geometric reconstruction assumed uniform buttress heights, the actual above-ground elevations of the vertical elements were refined by intersecting the structural model with the reconstructed Digital Terrain Model (DTM) developed in the previous phase. The resulting terrain-structure interaction was then resolved through a Boolean subtraction operation, enabling the definition of the

final geometry of the exposed structural components (Fig. 9). This procedure ensured geometric consistency between the dam model and the surrounding terrain.

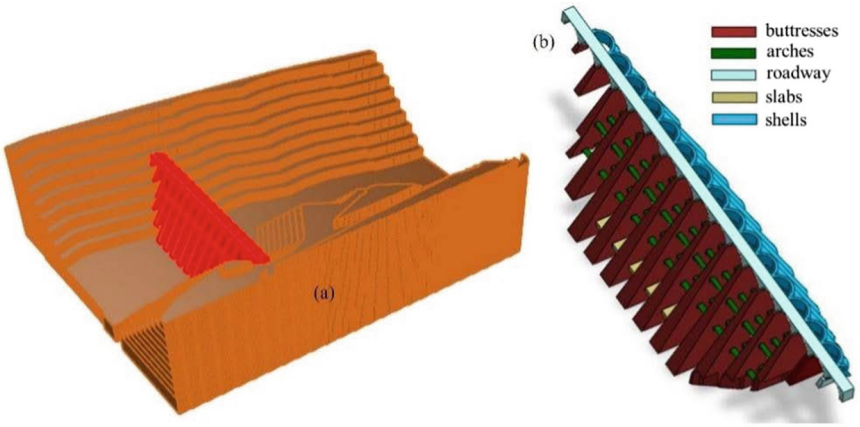

Fig. 9. (a) DTM and (b) geometry reconstruction of the dam.

Starting from this reconstructed geometry, a 3D finite element model (FEM) was implemented using Midas FEA software [28]. The mesh consists of 1264789 tetrahedral solid elements, each with a maximum size limited to 1 m (Fig. 10), ensuring an adequate level of detail for structural analysis.

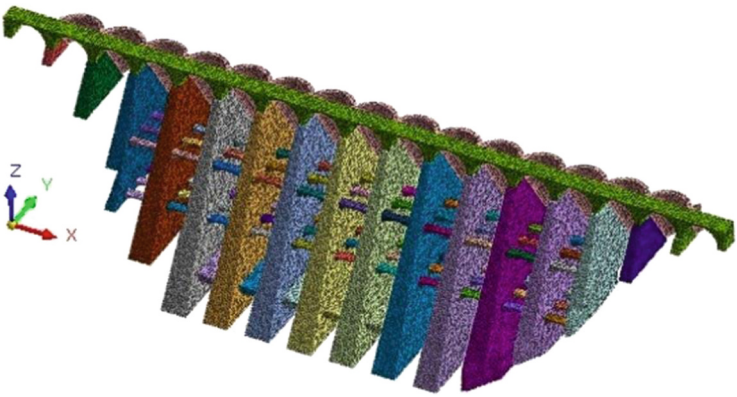

Fig. 10. Finite element model of the dam.

Boundary conditions were defined by applying fixed constraints at the base of the buttresses and along the soil–structure interfaces, assuming a perfectly restrained condition. Three types of loads were considered: (i) self-weight of the structure (automatically computed by the software), (ii) a crowd load applied on the roadway, equal to 4 kN/m^2 [29], and (iii) a horizontal load due to the presence of the water.

To account for the nonlinear behavior of both masonry and concrete, a smeared cracking (CSC) constitutive model was adopted for all materials [30], using the mechanical parameters reported in Table 1.

4.2 Numerical Analysis

The structural response of the dam was investigated through a non-linear static construction-stage analysis. The numerical procedure was implemented in two main phases. In the first phase, the structural model was generated by activating the elements and applying the self-weight together with the hydrostatic pressure of the reservoir, assumed to act up to two-thirds of the total height of the dam. In the second phase, the crowd load acting on the roadway was introduced through a load-stepping procedure, with sequential increments of 10% until the design load of 4 kN/m^2 specified in the rehabilitation project was reached. The resulting vertical displacements field at the end of the second phase is shown in Fig. 11.

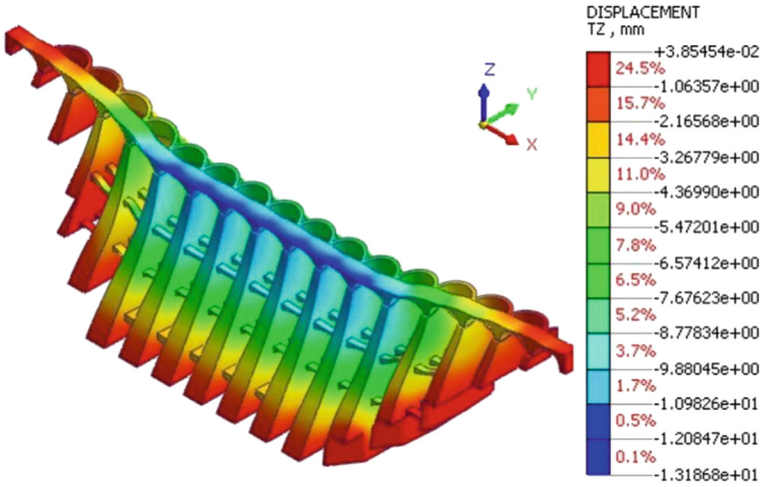

Fig. 11. Vertical displacements at the end of the second phase

The analysis indicates a maximum vertical displacement of approximately 1.32 cm (highlighted in blue), occurring at the central arch span. The displacement distribution is nearly symmetric with respect to the dam centerline, reflecting the regularity of the structural configuration and loading condition. The magnitude of the displacement remains within acceptable serviceability requirements, defined in the dam rehabilitation project, considering the overall length of the structure of approximately 257 m.

The corresponding stress fields, in terms of maximum tensile and compressive stresses, are reported in Figs. 7 and 8, respectively. The numerical results show that the stress field is largely consistent with the material strength capacities, with only limited localized regions exhibiting stress concentrations higher than the admissible limits. The maximum compressive stress is approximately 1 MPa, which is significantly lower

than the characteristic compressive strength of both masonry and concrete. This condition is primarily due to the dominance of the self-weight in the overall load combination, which largely exceeds the contribution of the crowd load (Figs. 12, 13 and 14).

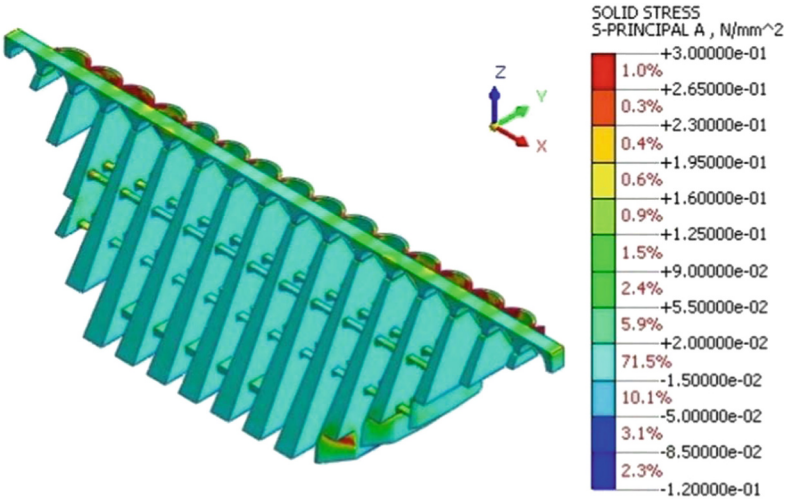

Fig. 12. Maximum tensile stress.

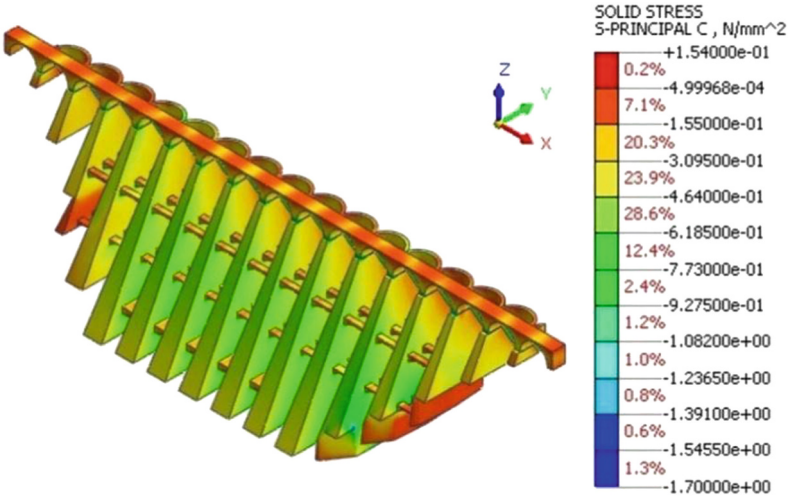

Fig. 13. Maximum compressive stress

Regarding tensile stresses, most areas of the dam remain within the tensile resistance of the materials. However, a few localized regions exhibit tensile stresses exceeding the masonry tensile strength, primarily concentrated in the upper portions of the structure.

This distribution is consistent with the observed structural condition, where cracking is mainly localized in these areas. Figure 9 illustrates the predicted cracking pattern in the masonry regions affected by tensile stress exceedance.

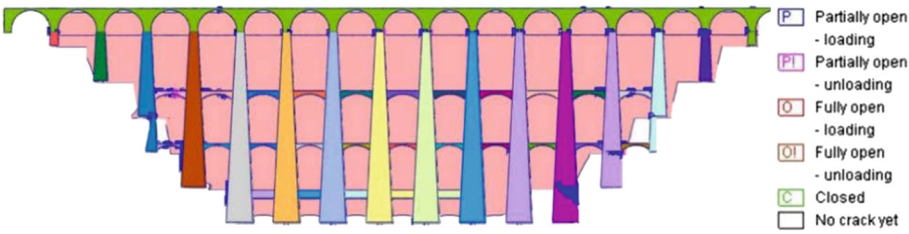

Fig. 14. Cracks distribution

The identified cracking patterns are limited to small, localized regions and are consistent with the principal tensile stress distribution, thus not posing significant concerns for the proposed adaptive reuse of the dam.

5 Conclusions

This study presents an integrated workflow combining GIS-based spatial analysis and structural modeling for the assessment and potential adaptive reuse of the Santa Chiara dam, a historical multiple-arch hydraulic structure.

A key challenge addressed in this work was the incomplete geometric characterization of the reservoir basin, particularly in submerged areas where direct bathymetric data were not available. To overcome this limitation, a simplified reconstruction methodology was developed, based on GIS spatial analysis, using publicly available DTMs, historical documentation, and geometric assumptions. The approach enabled the generation of a continuous and coherent model of the reservoir basin, suitable for subsequent numerical analyses, with the GIS environment acting as a bridge between largescale spatial data and structural modeling, ensuring a consistent transfer of geometrical information from the territorial to the structural scale.

The reconstructed terrain model was therefore successfully integrated into the structural modelling workflow, allowing the reliable definition of boundary conditions and load distributions. Indeed, unlike conventional approaches, where hydrostatic loads are often idealized or simplified, the adopted methodology enabled the explicit definition of the water domain.

The resulting finite element analysis highlighted an overall satisfactory structural behaviour of the dam under the loading conditions imposed by the rehabilitation project. Compressive stress (about 1 MPa) remains within acceptable limits across most of the structure, confirming the overall stability of the dam. Localized tensile stress exceedances and the associated cracking patterns, consistent with observed damage conditions, were found to be limited in extent and not critical for the global structural stability of the dam.

Overall, the results demonstrate that the proposed methodology provides a reliable approach for addressing incomplete geomorphological data in historical hydraulic

infrastructures. By integrating GIS-based reconstruction with structural modeling, the workflow ensures consistent geometric representation and reduces uncertainties related to complex and submerged morphologies. The reconstructed model directly informs the finite element model, enhancing the robustness and physical consistency of the simulations and improving the reliability of the results.

Finally, the proposed workflow is fully reproducible using widely available tools and can be easily applied to other historical hydraulic infrastructures where incomplete topographic or bathymetric data limit conventional analysis approaches. Future developments may include the integration of dedicated in situ measurements, such as bathymetric surveys, advanced remote sensing techniques, and more detailed modelling approaches supported by uncertainty-based simulations, to further refine the reconstruction of submerged geometries and improve the accuracy of the structural model.

Acknowledgments. The authors gratefully acknowledge Eng. Pierluigi Fenu for his contribution through his Bachelor's thesis, which supported the development of this research. The Municipality of Ula Tirso is also sincerely acknowledged for its collaboration and support.

Disclosure of Interests The authors have no competing interests to declare that are relevant to the content of this article.

References

1. Lopez-Bravo, C., Lopez, J.P.: Learning from medieval Italy: urban sustainability concepts from the heritage of hydraulic infrastructures. The cases of Venice, Siena and Bologna. J. Cult. Herit. Manag. Sustain. Dev. **16**(7), 111–126 (2026)
2. Abbozzo, A., Castori, G., Mirra, M., Speranzini, E.: Preserving templar heritage: a comprehensive structural assessment of the Church of San Bevignate in Perugia (Italy). Int. J. Archit. Herit., 1–25 (2026)
3. Colace, F., Limongiello, M., Lorusso, A., Pellegrino, M., Santaniello, D., Santoriello, A.: Digital twin for cultural heritage: a computational approach to predictive conservation. Digit. Appl. Archaeol. Cult. Herit. **40**, e00519 (2026)
4. Wang, L., Mao, Y., Cheng, Y., Liu, Y.: Deep learning-based diagnosing structural behavior in dam safety monitoring system. Sensors. **21**(4), 1171 (2021)
5. Fu, X., Wang, M., Zhao, G., Xu, Y., Qi, Y., Gu, G.: A method for characterizing and analyzing the structural behavior of concrete dams in cold regions. Sci. Rep. **16**, 2660 (2026)
6. Oliveira, S., Alegre, A., Carvalho, E., Mendes, P., Proença, J.: Seismic and structural health monitoring systems for large dams: theoretical, computational and practical innovations. Bull. Earthq. Eng. **20**, 4483–4512 (2022)
7. Fedele, R., Maier, G., Miller, B.: Health assessment of concrete dams by overall inverse analyses and neural networks. Int. J. Fract. **137**, 151–172 (2006)
8. Bretas, E.M., Lemos, J.V., Lourenco, P.B.: A DEM based tool for the safety analysis of masonry gravity dams. Eng. Struct. **59**, 248–260 (2014)
9. Nguyen-Tuan, L., Könke, C., Bettzieche, V., Lahmer, T.: Numerical modeling and validation for 3D coupled-nonlinear thermo-hydro-mechanical problems in masonry dams. Comput. Struct. **178**, 143–154 (2017)
10. Robles, L., Pena, F.: Influence of the mechanical properties of masonry in the structural behavior of gravity dams. Int. J. Archit. Herit. **16**(3), 415–427 (2022)

11. Chen, J. et al.: Study on inspection and recycling evaluation of stone masonry of old Kada dam after 46 years service. Case studies. Constr. Mater. **21**, e03545 (2024)
12. Associazione Italiana di Elettrotecnica, Elettronica, Automazione, Informatica e Telecomunicazioni (AEIT): L'Elettrotecnica, ISSN 1825-828X, vol. 103. AEIT (2017)
13. Careddu, N., Grillo, S.M.: "Trachytes" from Sardinia: Geoheritage and current use. Sustainability. **11**, 3706 (2019)
14. QGIS: Development Team: QGIS Geographic Information System (version 3.34). Open Source Geospatial Foundation Project. https://www.qgis.org. Accessed 01 Jan 2026
15. Agisoft Metashape Professional (version 2.2.2), Agisoft LLC, https://www.agisoft.com. Accessed 01 Jan 2026
16. Nocerino, E., Menna, F.: Photogrammetry: linking the world across the water surface. J. Mar. Sci. Eng. **8**, 128 (2020). https://doi.org/10.3390/jmse8020128
17. Westoby, M.J., Brasington, J., Glasser, N.F., Hambrey, M.J., Reynolds, J.M.: Structurefrom-motion' photogrammetry: a low-cost, effective tool for geoscience applications. Geomorphology. **179**, 300–314 (2012)
18. Klapa, P., Żygadło, A., Pepe, M.: 3D heritage reconstruction through HBIM and MultiSource data fusion: geometric change analysis across decades. Appl. Sci. **15** (2025). https://doi.org/10.3390/app15168929
19. Quadros, N.D., Collier, P.A., Fraser, C.S.: Integration of bathymetric and topographic LiDAR: a preliminary investigation. In: International Archives of Photogrammetry, Remote Sensing and Spatial Information Sciences (2008)
20. Yang, F., Qi, C., Su, D., Ding, S., He, Y., Ma, Y.: An airborne LiDAR bathymetric waveform decomposition method in very shallow water: a case study around Yuanzhi Island in the South China Sea. Int. J. Appl. Earth Obs. Geoinf. **109**, 102788 (2022)
21. U.S. Geological Survey Bathymetric Surveys: USGS bathymetric data and survey information. https://www.usgs.gov/faqs/where-can-i-find-bathymetric-data. Accessed 01 Jan 2026
22. NOAA National Bathymetric Source/Hydrographic Surveys: NOAA NOS hydrographic survey data. https://www.ncei.noaa.gov/products/nos-hydrographic-survey. Accessed 01 Mar 2026
23. GEBCO Shallow Water Bathymetry: GEBCO Global Bathymetric Grid and Shallow Water Data. https://www.gebco.net/data-products/gridded-bathymetry-data/shallow-water-bathymetry. Accessed 01 Jan 2026
24. Dey, S., Saksena, S., Merwade, V.: Assessing the effect of different bathymetric models on hydraulic simulation of rivers in data sparse regions. J. Hydrol. **575**, 838–851 (2019)
25. Regione Autonoma della Sardegna: Sardegna geoportale–regional spatial data infrastructure portal. https://www.sardegnageoportale.it/. Accessed 10 Mar 2026
26. Li, Z., Zhu, C., Gold, C.: Digital Terrain Modeling: Principles and Methodology. CRC Press, Boca Raton (2004)
27. Rhinoceros 8 user manual Robert McNeel & Associates (2025)
28. Midas FEA NX Analysis Reference (2025)
29. NTC: 2018 ministerial decree of 17 January 2018, official gazette of the Italian republic, No. 42, 20 February (2018)
30. Zucca, M., Reccia, E., Vecchi, E., Pintus, V., Dessì, A., Cazzani, A.: An evaluation of the structural behaviour of historic buildings under seismic action: a multidisciplinary approach using two case studies. Appl. Sci. **14**(22), 10274 (2024)